

# Pathogenic Mutations Located in the Hydrophobic Core of the Prion Protein Interfere with Folding and Attachment of the Glycosylphosphatidylinositol Anchor\*

Received for publication, November 5, 2004, and in revised form, December 10, 2004  
Published, JBC Papers in Press, December 10, 2004, DOI 10.1074/jbc.M412525200

Sophia Kiachopoulos, Andreas Bracher, Konstanze F. Winklhofer‡, and Jörg Tatzelt‡§

From the Department of Cellular Biochemistry, Max-Planck-Institute for Biochemie, D-82152 Martinsried, Germany

**Abnormal folding of the cellular prion protein (PrP<sup>C</sup>) is a key feature in prion diseases. Here we show that two pathogenic mutations linked to inherited prion diseases in humans severely affect folding and maturation of PrP<sup>C</sup> in the secretory pathway of neuronal cells. PrP-T183A and PrP-F198S adopt a misfolded and partially protease-resistant conformation, lack the glycosylphosphatidylinositol anchor, and are not complex glycosylated. These misfolded PrP mutants are not retained in the endoplasmic reticulum and are not subjected to the endoplasmic reticulum-associated degradation pathway. They rather are secreted, moreover, these mutants can be internalized by heterologous cells. Structural studies indicated that the side chains of Thr<sup>183</sup> and Phe<sup>198</sup> contribute to interactions between secondary structure elements in the C-terminal globular domain of PrP<sup>C</sup>. Consequently, we reasoned that a destabilized tertiary structure of these mutants could account for the defect in maturation. Indeed, mutations predicted to interfere selectively with the packing of the hydrophobic core of PrP<sup>C</sup> prevented the addition of the glycosylphosphatidylinositol anchor. Our study reveals that formation of the C-terminal globular domain of PrP<sup>C</sup> has an impact on membrane anchoring and indicates that misfolded secreted forms of the prion protein are linked to inherited prion diseases in humans.**

A hallmark of prion diseases in humans and animals is the conversion of the cellular prion protein (PrP<sup>C</sup>)<sup>1</sup> into a pathogenic conformation termed PrP<sup>Sc</sup> (reviewed in Refs. 1–4). Spontaneous misfolding of PrP<sup>C</sup> seems to be extremely rare based on the low incidence of sporadic prion diseases in humans (about 1 case in 1 million per year). However, inherited forms of the disease, some of which show a penetrance of nearly 100%, indicate that mutations within the prion protein gene can favor

the formation of a pathogenic conformer (5).

Biogenesis of PrP<sup>C</sup> is characterized by a series of post-translational modifications (reviewed in Ref. 6). During import into the endoplasmic reticulum (ER) the N-terminal signal peptide is cleaved and core glycans are attached to Asn<sup>180</sup> and Asn<sup>196</sup> of murine PrP (corresponds to Asn<sup>181</sup> and Asn<sup>197</sup> of human and Syrian hamster PrP) (7). Shortly after PrP<sup>C</sup> is fully translocated into the ER lumen, a glycosylphosphatidylinositol (GPI) anchor is transferred to Ser<sup>230</sup> (8). It is known that a single amino acid substitution in the GPI anchor signal sequence can significantly interfere with GPI anchor attachment (9), however, much less is known about the role of the protein conformation in this process. After the addition of the GPI anchor, both core glycans of PrP<sup>C</sup> are further processed in the Golgi compartment to generate a heterogeneous population of at least 52 different bi-, tri- and tetra-antennary glycans (10, 11).

Structural studies with recombinantly expressed PrP revealed a large flexibly disordered N-terminal region and a structured C-terminal domain (amino acids 126–226). This autonomously folding domain contains three  $\alpha$ -helical regions and a short two-stranded  $\beta$ -sheet (12–14). In a refined NMR analysis the precise structural definition of a large fraction of side chains was achieved and it became apparent that the globular domain of PrP<sup>C</sup> contains a tightly packed hydrophobic core (15).

An inherited prion disease in humans is linked to the amino acid substitution T183A, which destroys the first N-linked glycosylation acceptor site (16), raising the possibility that a defective glycosylation could favor the formation of pathogenic prion protein. However, structural studies revealed that the pathogenic mutation T183A (corresponds to T182A in mouse PrP<sup>C</sup>) destabilizes the hydrophobic core of the C-terminal globular domain, because it interferes with the formation of a hydrogen bond between helix 2 and the  $\beta$ -sheet (15). In the same study it was proposed that a different pathogenic mutation, F198S (17), could also destabilize the tertiary structure of the globular domain.

In this study we analyzed the biogenesis and maturation of PrP-T183A and PrP-F198S in the secretory pathway of neuronal cells and show that these pathogenic mutants spontaneously adopt a partially protease-resistant phenotype, lack the GPI anchor, and are secreted. A mechanistic analysis suggested that the defect in maturation is caused by the destabilization of the hydrophobic core, suggesting that the formation of the tertiary structure influences the efficiency of the GPI anchor attachment.

## EXPERIMENTAL PROCEDURES

**Generation of Wild-type (WT) PrP and PrP Mutants**—The coding region of the mouse PRNP modified to express PrP-L108M/V111M was inserted into the pcDNA3.1/Zeo vector (Invitrogen), allowing discrimination by monoclonal antibody 3F4 (18). Amino acid deletions and

\* This work was supported by Deutsche Forschungsgemeinschaft Grants TA 167/2, WI 2111/1, and SFB 596 and the Bayerische Staatsminister für Wissenschaft, Forschung und Kunst (for Prion, MPI3). The costs of publication of this article were defrayed in part by the payment of page charges. This article must therefore be hereby marked "advertisement" in accordance with 18 U.S.C. Section 1734 solely to indicate this fact.

‡ Both are considered senior authors.

§ To whom correspondence should be addressed: Dept. of Cellular Biochemistry, Max-Planck-Institute for Biochemie, Am Klopferspitz 18, D-82152 Martinsried, Germany. Fax: 49-89-8578-2211; E-mail: tatzelt@biochem.mpg.de.

<sup>1</sup> The abbreviations used are: PrP<sup>C</sup>, cellular prion protein; ER, endoplasmic reticulum; GPI, glycosylphosphatidylinositol; Endo H, endoglycosidase H; PNGase F, peptide N-glycosidase F; PBS, phosphate-buffered saline; PK, proteinase K; PI-PLC, phosphatidylinositol-phospholipase C; WT, wild type; ERAD, endoplasmic reticulum-associated protein degradation.

substitutions were introduced by PCR cloning techniques. The following amino acid substitutions were created: PrP-N180Q, PrP-T182A, PrP-F197S, PrP-V160S, and PrP-V160W. The C-terminal deletion in PrP-V160WΔGPI includes amino acids 230–254. For generation of cytosolic PrP (cytoPrP) the ER signal sequence (amino acids 2–22) was deleted. PrP-M204S was described earlier (19). All amino acid numbers refer to the mouse PrP sequence (GenBank™ accession number M18070).

**Antibodies**—The mouse monoclonal antibody 3F4 was described earlier (20) and purchased from Signet Pathology Systems (Dedham).

**Cell Lines, Transfections, Endo H, and Peptide N-Glycosidase F (PNGase F) Digestion**—Mouse N2a and human SH-SY5Y cells were cultivated as described (19, 21). Cells were transfected by a liposome-mediated method using Lipofectamine Plus reagent according to the manufacturer's instructions (Invitrogen). For Endo H digestion, protein lysates were adjusted to 0.5% SDS, boiled for 10 min, and then digested with endoglycosidase H (New England Biolabs) for 1 h at 37 °C, as specified by the manufacturer. For PNGase F digestion, aliquots of cell lysates (50 µg of protein) were digested with 1 unit of PNGase F (Roche) for 24 h at 37 °C. The reactions were stopped by the addition of Laemmli sample buffer.

**Proteasomal and Lysosomal Degradation Experiments**—For inhibition of proteasomal degradation cells were incubated with MG 132 (Calbiochem, dissolved in Me<sub>2</sub>SO) at the concentration and the time indicated. To inhibit lysosomal degradation, cells were incubated with bafilomycin A1 (Calbiochem, 1 µM, dissolved in Me<sub>2</sub>SO) for 16 h as described earlier (22).

**Assay for Uptake of Heterologous PrP**—Cell culture medium collected from transiently transfected N2a cells was filtered to remove possibly detached cells and then added to untransfected cells. After 48 h at 37 °C, these cells were lysed and heterologous PrP was detected by Western blotting using the monoclonal antibody 3F4. In parallel, cells were analyzed by indirect immunofluorescence.

**Detergent Solubility Assay, Secretion Analysis, and Proteolysis Experiments**—As described previously (23), cells were washed twice with cold PBS, scraped off the plate, pelleted by centrifugation, and lysed in cold buffer A (0.5% Triton X-100 and 0.5% sodium deoxycholate in PBS). The lysate was centrifuged at 15,000 × g for 20 min at 4 °C. After boiling in Laemmli sample buffer, supernatants and pellets were analyzed by immunoblotting. To examine the secretion of PrP into the cell culture supernatant, cells were cultivated in serum-free medium for 3 h at 37 °C. The medium was collected, PrP was precipitated with trichloroacetic acid and analyzed by Western blotting. For proteolysis experiments, cells were lysed in cold buffer A and incubated for 30 min at 4 °C with proteinase K (PK) (Roche) at the concentrations indicated. The reaction was terminated by addition of Pefabloc SC (Roche) and boiling in Laemmli sample buffer. Residual PrP was detected by Western blotting.

**Phospholipase C and Trypsin Treatment**—Cells were washed twice with ice-cold PBS and then maintained on ice. Phosphatidylinositol-phospholipase C (PI-PLC) (Roche) in PBS was added to the cells for 3 h at 4 °C (0.5 units/ml). Medium was collected, the cells were washed extensively with PBS and lysed in cold buffer A. Cellular PrP was analyzed by the detergent solubility assay. PrP present in the cell culture medium was precipitated by trichloroacetic acid and analyzed by Western blotting. For trypsin treatment, intact cells were washed twice with cold PBS and incubated at 4 °C in trypsin (0.25%, w/v) for 5 min. The reaction was terminated by the addition of soybean trypsin inhibitor (Invitrogen). The cells were collected by a brief centrifugation, washed with trypsin inhibitor, and analyzed with the detergent solubility assay.

**Western Blot Analysis**—Detergent-fractionated cell lysates were size fractionated by SDS-PAGE, and proteins were transferred to nitrocellulose (Protran BA 85, Schleicher & Schüll) by electroblotting as described earlier (24).

**Metabolic Labeling and Immunoprecipitation**—Cells were starved for 30 min in methionine-free modified Eagle's medium (Invitrogen) and subsequently labeled for 30 min with 300 µCi/ml Pro-mix L-[<sup>35</sup>S] *in vitro* cell label mixture (Amersham; >37 TBq/mmol) in methionine-free modified Eagle's medium. For the chase, the labeling medium was removed, the cells were washed twice and then incubated in complete medium for the times indicated. For Endo H digestion, immunoprecipitation products were adjusted to 0.5% SDS, boiled for 10 min, and digested with endoglycosidase H (New England Biolabs) for 1 h at 37 °C. Immunoprecipitation of PrP was performed as described previously (21) using the monoclonal antibody 3F4. Immunoprecipitation products were analyzed by SDS-PAGE. Gels were impregnated with Amplify (Amersham Biosciences) and exposed to film.

**Surface Biotinylation**—As described earlier (22), N2a cells grown in poly-D-lysine-coated (Sigma, 0.1 mg/ml) dishes were transiently transfected, washed twice with cold PBS, and labeled with impermeant LC-sulfo-NHS-(+)-biotin (Molecular BioSciences, 0.5 mg/ml) at 4 °C for 1 h. The cells were washed three times with cold PBS, incubated in ice-cold glycine (10 mM) at 4 °C for 30 min, and lysed in cold buffer A. PrP present in the detergent-soluble or -insoluble fraction was immunoprecipitated using monoclonal antibody 3F4. The immunoprecipitation products were analyzed by Western blotting using a streptavidin-horseradish peroxidase conjugate (Amersham Biosciences).

**Indirect Immunofluorescence**—N2a and SH-SY5Y cells grown on glass coverslips were rinsed two times in PBS, fixed in ice-cold methanol (permeabilized cells) for 10 min or in 3% paraformaldehyde (non-permeabilized cells) for 30 min, and incubated with monoclonal antibody 3F4 (dilution 1:200) in PBS containing 1% bovine serum albumin for 45 min at 37 °C. After extensive washing with cold PBS, an incubation with Cy3-conjugated anti-mouse antibody (Dianova) (dilution 1:200) followed at 37 °C for 30 min. The washed coverslips were mounted onto glass slides and examined by fluorescence microscopy (Axiovert 200 M, Zeiss) using the AxioVision 3.0 software.

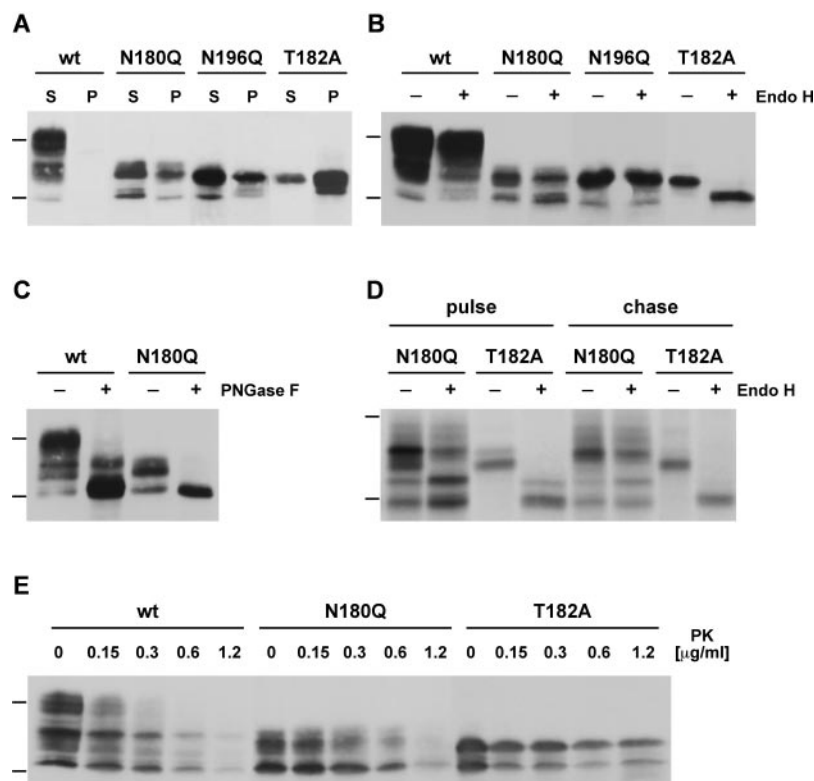
## RESULTS

**The Pathogenic PrP Mutant T182A Is Not Complex Glycosylated and Adopts a Partially Protease-resistant Conformation**—To analyze the biogenesis of pathogenic human PrP mutants in mouse neuroblastoma (N2a) cells, we cloned the mouse PrP equivalents. It should be noted that all residues affected by pathogenic mutations are conserved between human and mouse PrP. In mouse PrP, the numbering of the amino acids is changed by –1 in comparison to human PrP<sup>C</sup>; for example, the pathogenic human mutant T183A corresponds to T182A in mouse PrP. All PrP constructs analyzed in this study contain the epitope for monoclonal antibody 3F4, which does not react with endogenous mouse PrP (20).

We first addressed the question whether the lack of the first glycosylation site might change the biogenesis and cellular trafficking of PrP<sup>C</sup>. We therefore conducted a comparative study between T182A and N180Q, two mutants characterized by a defective consensus site for the first N-linked glycosylation. In addition, we included the N196Q mutant, in which the second glycosylation site is inactivated. After transient expression of these mutants in N2a cells, detergent lysates were prepared and fractionated by centrifugation. The Western blot analysis revealed that in contrast to wild type (WT) PrP, N180Q, and N196Q, the pathogenic mutant T182A was mainly found in the detergent-insoluble fraction (Fig. 1A). To analyze the glycosylation status of the PrP mutants, protein extracts were digested either with Endo H or PNGase F prior to the Western blot analysis. Whereas Endo H only cleaves high mannose or hybrid structures and is not active on glycans of complex structure, PNGase F can also deglycosylate fully matured PrP<sup>C</sup>. Consequently, WT PrP was not affected by Endo H digestion (Fig. 1B), but was deglycosylated by PNGase F (Fig. 1C). Similarly, N180Q and N196Q were resistant to Endo H, indicating that the remaining glycan was converted into a complex structure. In contrast, the glycan attached to T182A was sensitive to Endo H digestion, revealing that this mutant was not complex glycosylated (Fig. 1B). To investigate glycosylation of these PrP mutants in more detail, we performed metabolic labeling experiments and analyzed PrP by immunoprecipitation. During the chase, N180Q acquired an Endo H-resistant phenotype, whereas the glycan of the pathogenic mutant T182A remained fully sensitive to Endo H digestion, i.e. was not converted into a complex structure (Fig. 1D).

The finding that T182A was mainly present in the detergent-insoluble fraction (Fig. 1A) might indicate a misfolded conformation of this pathogenic mutant. To test this possibility, we performed limited proteolysis experiments. Protein extracts from transiently transfected cells were incubated with increasing amounts of PK and the remaining PrP was detected by

**FIG. 1. The pathogenic mutant T182A adopts a misfolded conformation, is not complex-glycosylated, and is partially protease-resistant.** N2a cells were transiently transfected with wild type PrP (*wt*) or PrP mutants lacking the first (N180Q and T182A) or the second (N196Q) glycosylation site, respectively. **A**, the pathogenic mutant T182A adopts a misfolded conformation. After cell lysis and centrifugation, PrP present in the detergent-soluble (*S*) and -insoluble (*P*) fraction was detected by Western blotting using monoclonal antibody 3F4. **B–D**, T182A is not complex glycosylated. **B** and **C**, the cell lysate was split into two aliquots. One aliquot was incubated with Endo H (**B**) or PNGase F (**C**), respectively, the other was mock-treated. PrP expression was then analyzed by Western blotting. **D**, transiently transfected N2a cells were metabolically labeled with [<sup>35</sup>S]methionine for 30 min and either analyzed directly (*pulse*) or incubated in fresh medium for 1 h (*chase*). Immunoprecipitation products were separated into two aliquots and incubated with or without Endo H. **E**, T182A adopts a partially protease-resistant conformation. Protein extracts from transiently transfected N2a cells were subjected to increasing concentrations of PK as indicated. The remaining PrP was detected by Western blotting. Molecular size markers are indicated as bars on the left side of the panels and represent 36 and 22 kDa.



Western blotting. WT PrP and the monoglycosylated mutant N180Q were sensitive to PK digestion in a similar manner, however, the pathogenic mutant T182A was stable at a PK concentration sufficient to completely degrade WT PrP and N180Q (Fig. 1E).

The initial analysis revealed that two PrP mutants, which both lack the first glycosylation site, display distinct biochemical properties. Whereas the remaining glycan of N180Q is converted into a complex structure, the core glycan of T182A is not terminally processed. In addition, the pathogenic mutant T182A adopts a misfolded, partially PK-resistant conformation.

**T182A Is Not Present at the Plasma Membrane**—In a next step we analyzed the cellular localization of the PrP mutants. Intact cells were incubated either with trypsin to remove all cell surface proteins (Fig. 2A), or with PI-PLC to specifically liberate GPI-anchored proteins (Fig. 2B). Both assays were performed at 4 °C to prevent possible secretion. After trypsin treatment lysates prepared from WT PrP- or N180Q-expressing cells had lost most of their PrP, indicating that it was localized at the cell surface (Fig. 2A, *Trypsin* +). Similarly, after PI-PLC treatment WT PrP and N180Q were found almost quantitatively in the cell culture supernatant (Fig. 2B, *PIPLC* +, *Medium*). In contrast, the relative amount of T182A present in extracts prepared from trypsin- or PI-PLC-treated cells was not reduced when compared with the mock-treated control, nor was the cell culture supernatant of PI-PLC-treated cells expressing T182A enriched in PrP. Notably, in both assays the phenotype of T182A was similar to M204S, a PrP mutant generated and characterized in a previous study from our group (19). The single amino acid substitution in M204S destabilizes an interaction of helix 3 with helix 1. As a consequence, M204S does not receive a GPI anchor, the core glycans are not converted into complex structures, and the mutant protein is secreted into the cell culture medium (19).

To provide further evidence that T182A was not present at the plasma membrane, we incubated the cells with the plasma

membrane impermeant reagent LC-sulfo-NHS-(+)-biotin to specifically label cell surface PrP. After biotinylation, the cells were lysed in detergent buffer and PrP present in the detergent-soluble and -insoluble fraction was purified by immunoprecipitation with the anti-PrP antibody 3F4. Biotinylated PrP was then detected by Western blotting using streptavidin coupled to horseradish peroxidase. As shown in the left panel of Fig. 2C, only WT PrP and N180Q were biotinylated, indicating localization at the cell surface. To control expression of T182A, we analyzed a small fraction of the lysates prior to immunoprecipitation by Western blotting using the anti-PrP antibody 3F4 (Fig. 2C, right panel).

Finally, we examined the cellular localization of the different PrP mutants by indirect immunofluorescence experiments. For this approach we used mouse N2a cells as well as the human neuroblastoma cell line SH-SY5Y, which does not express detectable amounts of endogenous PrP<sup>C</sup> (data not shown). To prove the cell surface localization of PrP, we first performed immunofluorescence experiments in non-permeabilized cells. Supporting the biochemical data, only WT PrP and N180Q were detectable with this approach (Fig. 3A). After permeabilization of the cells, T182A was visualized, indicating the intracellular localization of the pathogenic mutant (Fig. 3B).

**T182A Is Secreted into the Cell Culture Medium and Can Be Internalized by Heterologous Cells**—The analysis described above revealed that the remaining glycan of the pathogenic mutant T182A was not converted into a complex structure and that the mutant protein was not present at the plasma membrane. These results mainly corroborate earlier reports that were interpreted such that T182A was not transported through the secretory pathway but retained in the ER (25, 26). Indeed, Endo H-sensitive glycans are often used as a diagnostic marker for proteins residing in the ER, however, numerous examples indicate that complex glycosylation is dispensable for trafficking of PrP. A PrP mutant devoid of the GPI anchor signal sequence (PrPΔGPI) is mainly unglycosylated, yet efficiently secreted into the cell culture medium (19, 27, 28). Similarly,



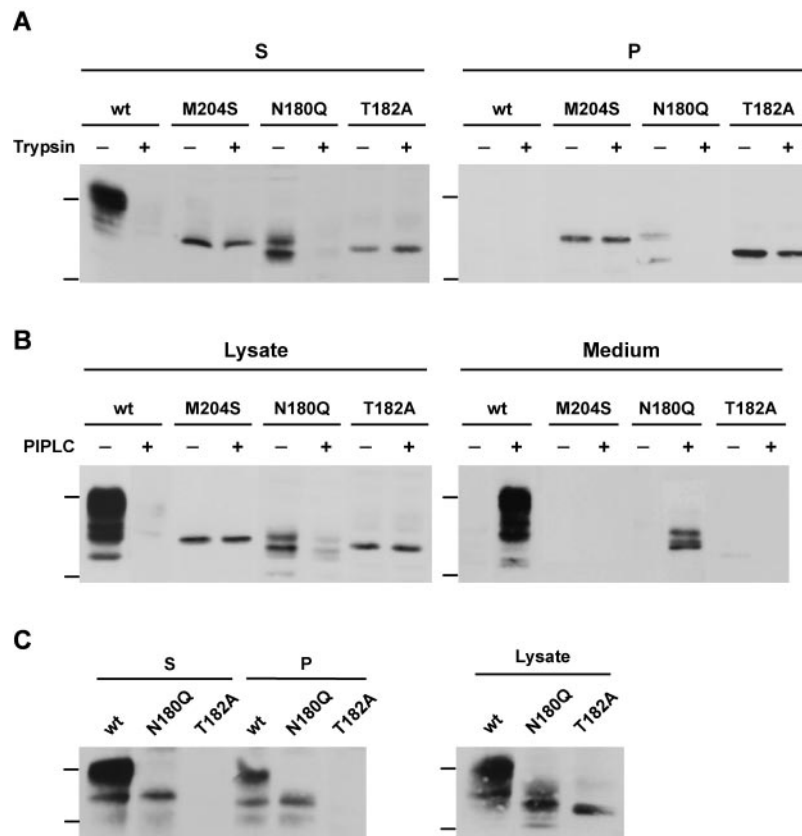


**FIG. 2. T182A is not present at the plasma membrane.** N2a cells were transiently transfected either with wild type PrP (*wt*), with PrP mutants lacking the first glycosylation site (N180Q and T182A), or with PrP-M204S, a mutant with a disrupted hydrophobic interaction between helix 3 and helix 1 (19). **A**, intact cells were incubated on ice with trypsin to remove cell surface proteins. As a control, mock-treated cells (*Trypsin* –) were analyzed in parallel. After cell lysis and centrifugation, residual PrP present in the detergent-soluble (*S*) and -insoluble (*P*) fraction was detected by Western blotting. **B**, live cells were incubated at 4 °C with phospholipase C (*PI-PLC* +) to release GPI-anchored proteins from the cell surface or mock-treated (*PI-PLC* –). PrP present in the cell lysate (*Lysate*) or cell culture supernatant (*Medium*) was detected by Western blotting. **C**, biotinylation of cell surface PrP. Transiently transfected live cells were incubated with a plasma membrane impermeable biotinylation agent. After biotinylation cells were lysed and PrP present in the detergent-soluble (*S*) or -insoluble (*P*) fraction was purified by immunoprecipitation with anti-PrP antibody 3F4. The immune pellet was analyzed by Western blotting using a streptavidin-horseradish peroxidase conjugate (*left panel*). As a control for PrP expression, a small aliquot of the whole lysate was taken prior to immunoprecipitation and analyzed by Western blotting using the anti-PrP antibody 3F4 (*right panel*). Molecular size markers are indicated as *bars* on the *left side* of the panels and represent 36 and 22 kDa.

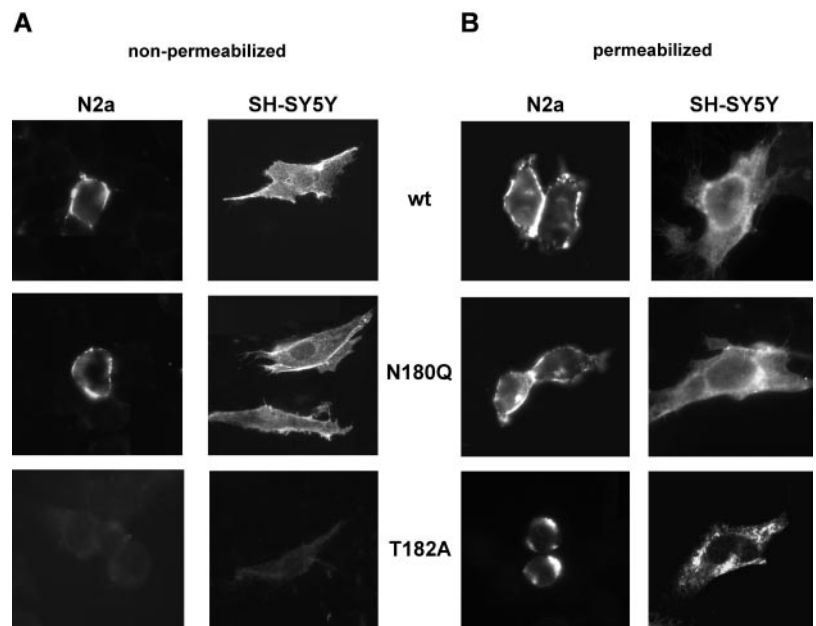
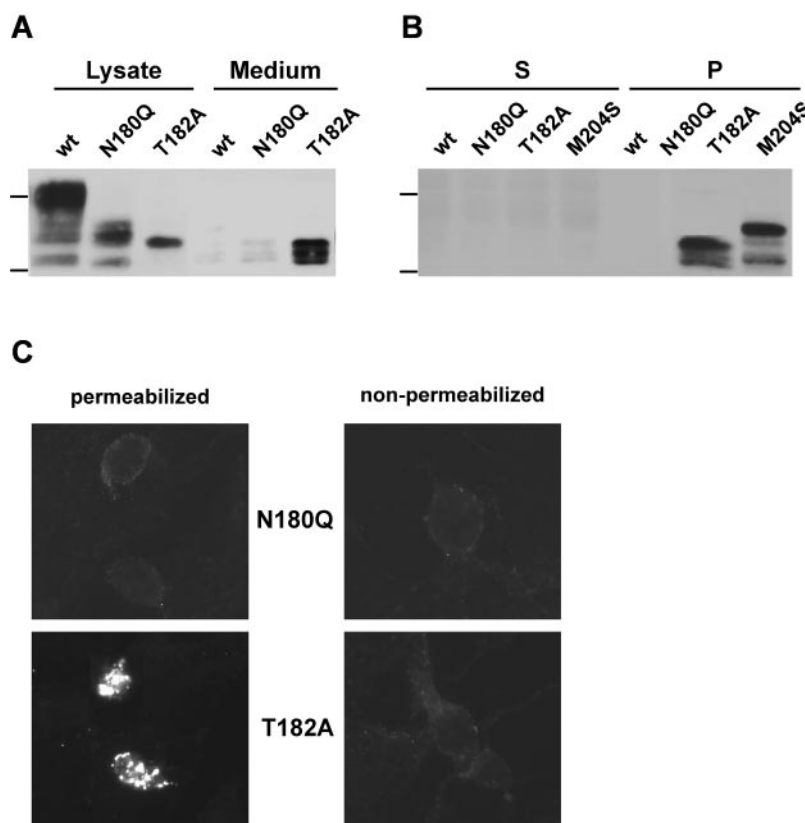


**FIG. 3. Cellular localization of PrP in intact cells.** SH-SY5Y or N2a cells grown on glass coverslips were transiently transfected either with wild type PrP (*wt*) or N180Q or T182A. Localization of PrP was visualized by indirect immunofluorescence of non-permeabilized (**A**) and permeabilized cells (**B**) using the monoclonal antibody 3F4.

high mannose glycoforms of different PrP mutants, such as M204S, are efficiently secreted (19). Even trafficking of GPI-anchored PrP<sup>C</sup> is not dependent on the formation of complex

glycans. In the presence of geldanamycin or  $\alpha$ -mannosidase inhibitors, a high mannose isoform of PrP<sup>C</sup> is present on the plasma membrane (29).

**FIG. 4. T182A is secreted into the cell culture medium and can be internalized by heterologous cells.** *A*, T182A is secreted into the cell culture medium. Transiently transfected cells were cultivated in serum-free medium for 3 h at 37 °C. PrP present in the cell lysate (*Lysate*) or cell culture medium (*Medium*) was detected by Western blotting. *B* and *C*, secreted T182A can be internalized by heterologous cells. Cell culture medium collected from cells transiently transfected with WT PrP, M204S, N180Q, and T182A was filtered and added to untransfected N2a cells. After further incubation at 37 °C for 48 h, these cells were analyzed as described below. *B*, secreted T182A is detectable in the detergent-insoluble fraction of heterologous cells. After cell lysis, PrP present in the detergent-soluble (*S*) or -insoluble (*P*) fraction was analyzed by immunoblotting using the 3F4 antibody. *C*, cellular localization of internalized T182A in intact heterologous cells. PrP was analyzed by indirect immunofluorescence of permeabilized and non-permeabilized N2a cells as described in the legend to Fig. 3. Molecular size markers are indicated as bars on the left side of the panels and represent 36 and 22 kDa.



Based on these findings we investigated possible secretion of T182A. Transiently transfected cells were cultivated in serum-free medium for 3 h at 37 °C and then the cell culture supernatant was analyzed for the presence of PrP. Indeed, the pathogenic mutant was efficiently secreted under these conditions, in contrast to WT PrP and N180Q (Fig. 4*A*, *Medium*). What might be the fate of secreted T182A? To address this question, we collected cell culture medium from transfected cells, removed possibly detached cells and added this cell-free medium to untransfected N2a cells. After 48 h at 37 °C, these cells were extensively washed, lysed, and PrP present in the detergent-soluble and -insoluble fractions was analyzed by Western blotting using the 3F4 antibody (Fig. 4*B*). Neither WT PrP nor the monoglycosylated mutant N180Q was present in the cell extracts, however, the T182A mutant could be detected in the detergent-insoluble fraction of the heterologous cells, similarly to M204S, which is efficiently secreted as well (19). To specifically investigate whether the pathogenic PrP mutant simply associated with the cell surface of the heterologous cells or was present within the cells, we performed indirect immunofluorescence experiments with permeabilized and non-permeabilized cells using the 3F4 antibody (Fig. 4*C*). 3F4-positive cells were found only in untransfected N2a cells incubated in medium derived from T182A-expressing cells. Moreover, T182A was detectable exclusively in permeabilized cells, indicating an intracellular localization.

These experiments revealed that misfolded T182A is not retained in the ER. This pathogenic mutant is rather efficiently secreted, moreover, it can be internalized by heterologous cells.

**T182A Is Degraded in a Lysosomal Compartment**—The foregoing experiments revealed that T182A adopts a misfolded conformation in the ER and, at least a fraction thereof, is secreted. Next we wanted to analyze the degradation pathway of T182A. It is known that misfolded ER proteins can be degraded via a pathway termed ER-associated protein degradation (ERAD). This pathway includes retrograde transport of the

misfolded proteins into the cytosol and subsequent degradation by the proteasome. To address the possibility that misfolded T182A is subjected to ERAD, we analyzed the effect of the proteasomal inhibitor MG132 on the lifetime of mutant PrP (Fig. 5*A*). As a control we included a cytosolic version of PrP into our analysis (cytoPrP), which is devoid of the N-terminal ER signal peptide and thus is targeted exclusively to the cytosol (30). Transiently transfected N2a cells were metabolically labeled with [<sup>35</sup>S]methionine for 30 min and then PrP was analyzed by immunoprecipitation either directly (pulse) or after an additional 2 h in fresh medium (chase). Cytosolically located PrP was efficiently degraded by the proteasome; in the presence of the proteasomal inhibitor MG132 cytoPrP was significantly stabilized (Fig. 5*A*, *cytoPrP*). However, proteasomal inhibition did not increase the relative amount of T182A present after the 2-h chase (Fig. 5*A*, *T182A*). Similar results were obtained in transiently transfected SH-SY5Y cells analyzed under steady state conditions (Fig. 5*B*).

Next we analyzed whether T182A is degraded in a lysosomal compartment. To interfere with lysosomal degradation, we used bafilomycin A1, an inhibitor of the vacuolar-type H<sup>+</sup>-ATPase (31). Indeed, interfering with lysosomal degradation increased the relative amount of the mutant T182A (Fig. 5*C*, *T182A*). Of note, WT PrP is also degraded in a lysosomal compartment, whereas cytoPrP is not subjected to lysosomal degradation (Fig. 5*C*, *wt*, *cyto*). Thus, misfolded T182A seems not to be subjected to ERAD but is rather degraded in a lysosomal compartment.

**Destabilization of the Globular Domain of PrP<sup>C</sup> Prevents GPI Anchor Attachment and Complex Glycosylation**—In both mutants N180Q and T182A the first N-linked glycosylation site is inactivated, however, the comparative study presented above revealed distinct phenotypes; only the pathogenic mutant T182A showed a severe defect in folding and maturation. Based on these findings we concluded that the phenotype of T182A cannot be attributed to the lack of the first N-linked glycan.

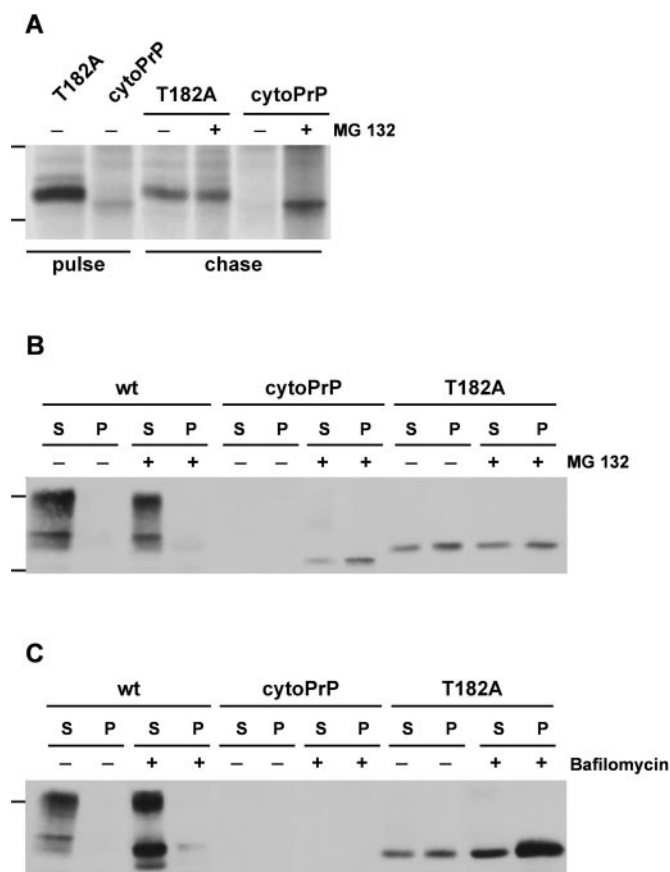


**FIG. 5. T182A is not degraded by the proteasome, but in lysosomal compartments.** SH-SY5Y or N2a cells were transiently transfected with wild type PrP (wt), T182A, and a PrP mutant lacking the ER signal sequence (cytoPrP). **A** and **B**, T182A is not degraded by the proteasome. **A**, N2a cells were metabolically labeled with [<sup>35</sup>S]methionine for 30 min and either analyzed directly (pulse) or after an additional 2 h in fresh medium (chase). To inhibit proteasomal degradation cells were cultivated during the pulse and the chase in the presence of the proteasomal inhibitor MG132 (50  $\mu$ M). **B**, transiently transfected SH-SY5Y cells were incubated for 3 h with MG 132 (30  $\mu$ M) or mock-treated, and PrP present in the detergent-soluble (S) and -insoluble (P) fraction was detected by Western blotting. **C**, T182A was degraded in lysosomal compartments. Transiently transfected SH-SY5Y cells were incubated for 16 h in cell culture medium supplemented with bafilomycin (1  $\mu$ M), or mock-treated. PrP present in the detergent-soluble (S) and -insoluble (P) fraction was detected by Western blotting. Molecular size markers are indicated as bars on the left side of the panels and represent 36 and 22 kDa.

The refined NMR structure of the recombinant PrP domain (amino acids 121–231) revealed that the side chain of Thr<sup>183</sup> (corresponds to mouse Thr<sup>182</sup>) is in hydrogen-bond contact to the carbonyl group of Cys<sup>179</sup> and to the amide group of Tyr<sup>162</sup> (Fig. 6, **A** and **B**) (15). This polar contact between  $\alpha$ -helix 2 and  $\beta$ -strand 2 presumably orientates and stabilizes the small  $\beta$ -sheet in PrP, which shields the hydrophobic core from the solvent. The pathogenic mutation T183A should weaken this interaction significantly. Indeed, *in vitro* experiments with purified recombinant PrP indicated that the pathogenic mutant T183A has a significantly decreased thermodynamic stability (32). It therefore was tempting to speculate that the folding defect we observed for mouse T182A in the secretory pathway of neuronal cells was because of a destabilization of the protein fold. To test this hypothesis experimentally, we left  $\alpha$ -helix 2 intact, but destabilized the hydrophobic packing against  $\beta$ -strand 2 by introducing mutations at position 161. In the refined NMR structure, the side chain of Val<sup>161</sup> is deeply buried in the hydrophobic core of the protein at the interface of  $\alpha$ -helices 2 and 3 and  $\beta$ -strand 2 (Fig. 6B) (15). Mutation to Ser

should impair these tight hydrophobic interactions; mutation to the bulky residue Trp is expected to abolish the interactions with the helices completely.

The biochemical analysis in transiently transfected N2a cells supported our hypothesis that a destabilization of the hydrophobic core interfered with the maturation of PrP<sup>C</sup>. The mouse V160S mutant was predominantly and the V160W mutant was exclusively Endo H-sensitive, indicating immature high mannose glycoforms (Fig. 7, **A** and **D**). Both mutants were secreted into the cell culture medium, *i.e.* they were not GPI-anchored (Fig. 7B). To specifically analyze whether the C-terminal GPI anchor signal peptide was cleaved, we generated V160W $\Delta$ GPI, a construct devoid of C-terminal amino acids 230–254. Metabolic labeling experiments revealed that the  $\Delta$ GPI construct was core glycosylated but appeared slightly smaller on SDS-PAGE, indicating that the GPI anchor signal peptide of V160W was not cleaved (Fig. 7, **C** and **D**). These findings present experimental evidence that formation of the tertiary structure seems to be a prerequisite for the maturation of PrP<sup>C</sup> in the secretory pathway of neuronal cells. Whereas attachment of the core glycans is not impaired by mutations destabilizing the globular fold of PrP<sup>C</sup>, GPI anchoring and the terminal processing of the core glycans do not occur.

**Another Pathogenic PrP Mutant, F197S, Spontaneously Adopts a Misfolded Conformation and Is Secreted**—Encouraged by these results, we included F198S in our analysis, a different pathogenic PrP mutant associated with inherited prion diseases in humans. Previous NMR studies revealed that the Phe to Ser substitution at position 198 could destabilize the hydrophobic core. Support for this prediction was obtained *in vitro*, indicating a significantly decreased thermodynamic stability of recombinant F198S (32, 33).

Our expression analysis in N2a cells revealed that F197S (the mouse equivalent of human F198S) shows a phenotype similar to T182A. The F197S mutant received core glycans, however, only a small fraction was converted into complex structures (Fig. 8A). Moreover, the majority of the mutant protein did not receive a GPI anchor and was efficiently secreted into the cell culture medium (Fig. 8, **B** and **C**). Similarly to the pathogenic mutant T182A, F197S adopted a detergent-insoluble conformation (data not shown). Consequently, we performed limited proteolysis experiments. Protein extracts from transiently transfected cells were incubated with increasing amounts of PK and the remaining PrP was detected by Western blotting. Indeed, the pathogenic mutant F197S was stable at a PK concentration sufficient to completely degrade WT PrP (Fig. 8D). This analysis revealed that F197S, a different mutant linked to inherited prion disease in humans, spontaneously adopts a misfolded conformation, lacks the GPI anchor, and is secreted as a high mannose glycoform.

## DISCUSSION

The formation of abnormally folded isoforms of the prion protein is the characteristic feature of prion diseases in humans and animals. We analyzed folding and maturation of PrP in the secretory pathway of neuronal cells and show that two different mutants linked to inherited prion diseases in humans spontaneously adopt a misfolded and partially protease-resistant conformation. In addition, the pathogenic mutants were characterized by a severe defect in their maturation. Instead of being GPI-anchored and complex glycosylated, the mutants were devoid of a membrane anchor and were secreted as high mannose glycoforms (Fig. 9). A mechanistic analysis revealed that mutations predicted to interfere with the formation of the hydrophobic core are characterized by a similar defect in folding and maturation. Our study shows that misfolded pathogenic PrP mutants can be secreted and indicates a link between

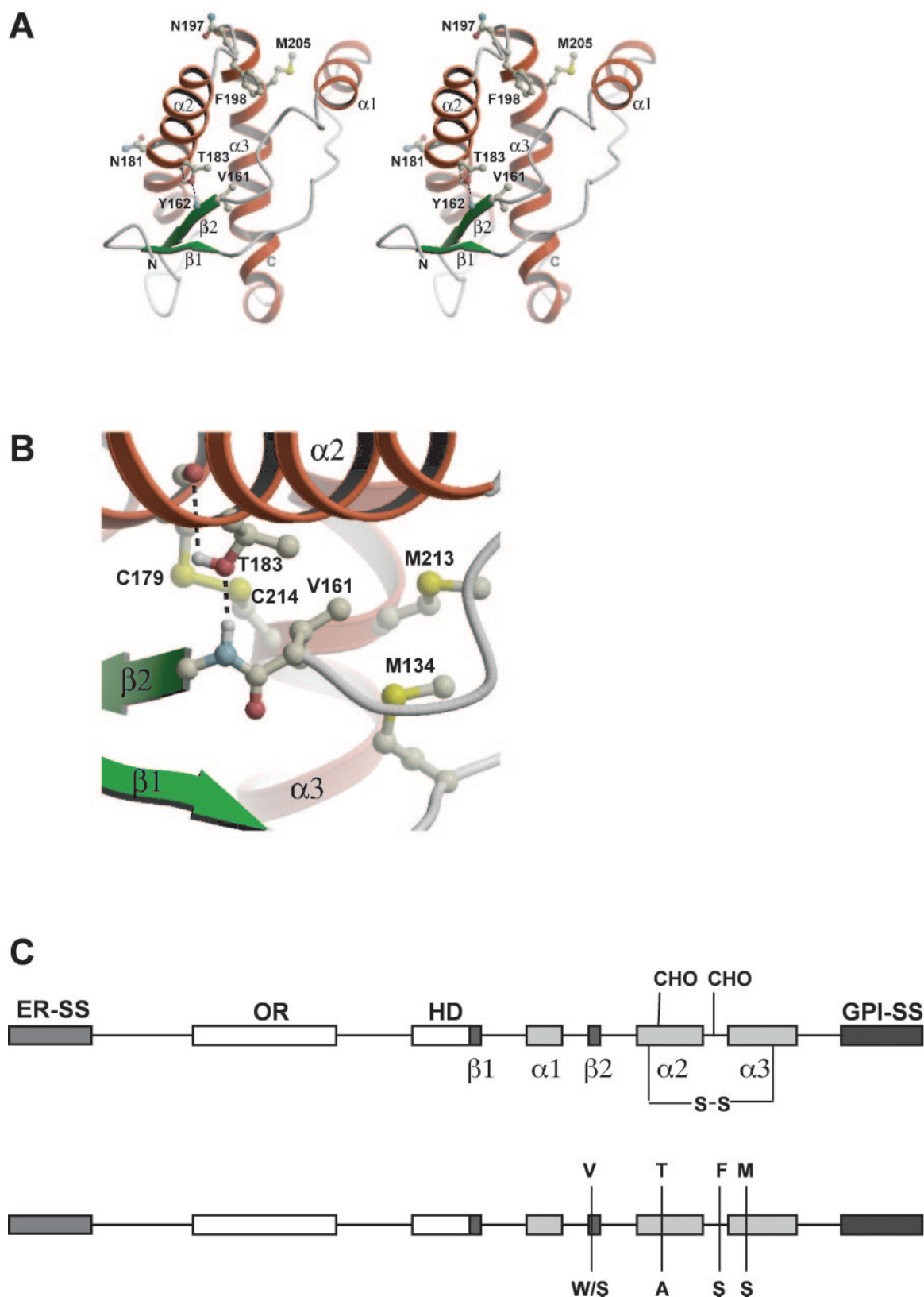


**FIG. 6. The side chains of Thr<sup>183</sup> and Phe<sup>198</sup> stabilize the hydrophobic core of the C-terminal globular domain.** *A*, the refined NMR structure of the C-terminal globular domain as a ribbon diagram in stereo representation. The side chains of residues discussed in the text are labeled and shown in ball-and-stick representations. Val<sup>161</sup>, Phe<sup>198</sup>, and Met<sup>205</sup> are components of the hydrophobic core. Thr<sup>183</sup> connects  $\alpha$ -helix 2 with the  $\beta$ -sheet by a hydrogen bond. Hydrogen atoms not involved in hydrogen bonding have been omitted for clarity. N181 and N197 are the acceptor sites for the carbohydrate moieties. Carbon, nitrogen, oxygen, and sulfur atoms are shown in gray, blue, red, and yellow, respectively. Hydrogen bonds are indicated by dashed lines. The chain termini are labeled. *B*, close-up of the hydrophobic pocket surrounding the side chain of Val<sup>161</sup>. The residues Met<sup>134</sup>, Val<sup>161</sup>, Met<sup>213</sup>, and Cys<sup>214</sup> form part of the hydrophobic core of PrP. Color coding and representation are as in panel *A*. Panels *A* and *B* were created with Protein Data Bank code 1AG2 (15) using the programs Molscript (46) and Raster3D (47). *C*, schematic representation of wild type PrP (*upper drawing*) and the PrP mutants analyzed (*lower drawing*): V161W/V161S, T183A, F198S, and M205S. The amino acid numbering refers to human PrP<sup>C</sup>. ER-SS, ER signal sequence; OR, octarepeat; HD, hydrophobic domain;  $\alpha$ 1–3, helical regions;  $\beta$ 1 and  $\beta$ 2,  $\beta$ -strands; CHO, N-linked glycan attachment sites; S-S, disulfide bond; GPI-SS, GPI signal sequence.



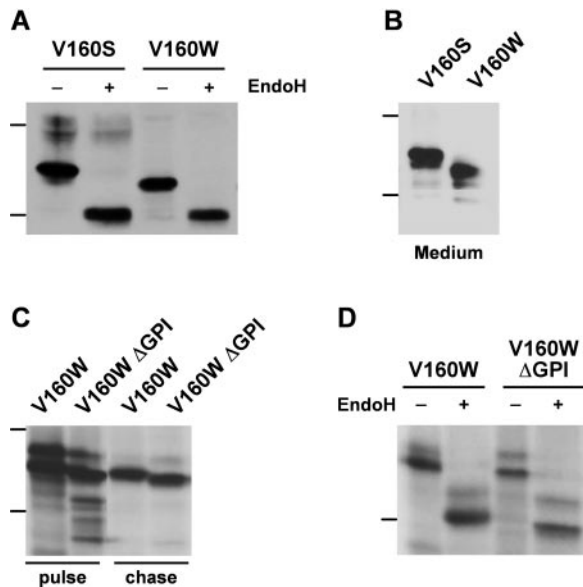


**FIG. 7. Destabilization of the hydrophobic core of the C-terminal globular domain interferes with GPI anchor addition and complex glycosylation.** N2a cells were transiently transfected with PrP mutants (V160S, V160W, or V160WΔGPI) designed to destabilize the globular domain of PrP. *A* and *B*, destabilization of the hydrophobic core interferes with complex glycosylation and GPI anchor attachment. N2a cells were transiently transfected with PrP mutants V160S or V160W. *A*, cells were lysed and the extract was split into two aliquots. One aliquot was incubated with Endo H, the other was mock-treated. PrP was analyzed by Western blotting. *B*, the transfected cells were cultivated in serum-free medium for 3 h at 37 °C. PrP present in the cell culture medium (*Medium*) was detected by Western blotting. *C* and *D*, the mutant V160W has an uncleaved GPI anchor signal peptide. N2a cells were transiently transfected with V160W or V160WΔGPI, a mutant with a deleted C-terminal GPI anchor signal sequence. Cells were metabolically labeled with [<sup>35</sup>S]methionine for 30 min and analyzed by immunoprecipitation using the 3F4 antibody. *C*, cells were either analyzed directly (*pulse*) or further incubated in fresh medium for 1 h (*chase*). *D*, immunoprecipitation products were divided into two aliquots and incubated with or without Endo H prior to SDS-PAGE analysis. Molecular size markers are indicated as bars on the left side of the panels and represent 36 and 22 kDa.

protein folding and GPI anchor addition.

**Pathogenic PrP Mutants Are Secreted and Can Be Internalized by Heterologous Cells**—With the discovery of monogenic familial forms of human prion diseases the pivotal role of the prion protein in the pathogenesis was emphasized; all cases analyzed so far are linked to mutations in the gene encoding the prion protein. In this study we show that two pathogenic missense mutations result in the generation of a misfolded and secreted form of the prion protein. In comparison to GPI-anchored wild type PrP<sup>C</sup>, the secreted PrP mutants were characterized by distinct biochemical properties. They spontaneously adopted a detergent-insoluble conformation and showed an increased resistance to a limited proteinase K digestion. Furthermore, the secreted PrP conformers were core glycosylated, however, the high mannose glycans were not processed into complex glycans. Interestingly, high mannose glycoforms of PrP<sup>C</sup> are preferred substrates for the conversion into PrP<sup>Sc</sup> (29).

How can the pathogenic potential of the misfolded PrP mutants be explained? Two scenarios are conceivable. First, misfolded PrP in the ER imposes stress on the affected cells. Second, secreted misfolded PrP interacts with components on the plasma membrane or along the endocytic pathway. Misfolded proteins within the ER can activate the unfolded protein response and can be degraded via the ERAD pathway (34). However, we could not detect induction of the unfolded protein response by misfolded PrP conformers in the secretory pathway

of neuronal or yeast cells (19, 35). Similarly, we did not observe that significant fractions of the misfolded mutants T182A or F197S were degraded by the proteasome. Thus, misfolded PrP seems not to induce ER stress, at least in dividing cells grown in culture. On the other hand, it is conceivable that the apparent lack of an efficient quality control contributes to or enhances the pathogenic potential of misfolded PrP, because it allows misfolded PrP to be secreted and to interact with heterologous cells. Such an impairment of cellular quality control systems to recognize and eliminate misfolded PrP not only favors the build-up of misfolded mutant PrP. Similarly, misfolded isoforms of wild type PrP as well as PrP<sup>Sc</sup> would escape cellular degradation and could accumulate. In this context it is interesting to note that in scrapie-infected N2a cells the cellular stress response is impaired (36, 37).

Our results demonstrate that misfolded PrP transits through the secretory pathway, is long-lived, and can be internalized, suggesting that the pathogenic conformers could interact with various cellular components present at the cell surface or within the endocytic pathway. In this context it is important to note that T182A is present in a lysosomal compartment where wild type PrP<sup>C</sup> is also found.

**Protein Folding and GPI Anchor Addition**—Our study not only provides a mechanistic analysis of pathogenic prion mutants, it also indicates an interplay between protein folding and the addition of a GPI anchor. We observed that mutations that are predicted to destabilize the globular domain of PrP<sup>C</sup> interfere with the addition of the GPI anchor. Notably, cleavage of the signal peptide and core glycosylation, two modifications that occur prior to the transfer of the GPI anchor, were not affected. Cleavage of the N-terminal ER signal peptide and the addition of the core glycans take place during translocation of the nascent chain. Recently, it has been shown that the C-terminal GPI anchor signal sequence does not serve as a transmembrane domain, providing experimental evidence that the protein is fully translocated into the ER lumen prior to GPI anchor addition (38). Based on *in vitro* data showing that folding of the globular domain of PrP<sup>C</sup> is extremely fast (39), it is conceivable that PrP adopts a tertiary structure prior to addition of the GPI anchor. Mutant PrP might fold into an alternate tertiary structure, burying the GPI anchor signal sequence. An impact of protein folding on a different post-translational modification has been shown in previous studies, indicating that the structure of the nascent chain determines the efficiency of N-linked glycosylation (40, 41).

Why do we think that the defective GPI anchor attachment is linked to an alteration in the tertiary structure of the prion protein? The main argument is that an impact of the pathogenic mutations on the secondary structure of PrP does not seem plausible. In addition, we designed mutations that specifically destabilized the hydrophobic core of the prion protein. As predicted, V160S, V160W, and M204S severely affected the maturation of PrP, similarly to the pathogenic mutations T182A and F197S. Indirect evidence was obtained from the analysis of N180Q and N196Q. These mutations seem not to affect the stability of the hydrophobic core and hence, the maturation of the mutant proteins is not impaired. Finally, our results are in line with previous *in vitro* experiments. Based on a refined NMR structure, it was predicted that the two pathogenic mutations T183A and F198S would specifically destabilize the globular domain (15). Indeed, *in vitro* experiments with recombinant T183A and F198S provided experimental evidence that both mutations destabilize the mutant protein. Moreover, it was shown that F198S has an increased propensity to adopt a scrapie-like conformation (32, 33).

In addition to the defective GPI anchor attachment, the



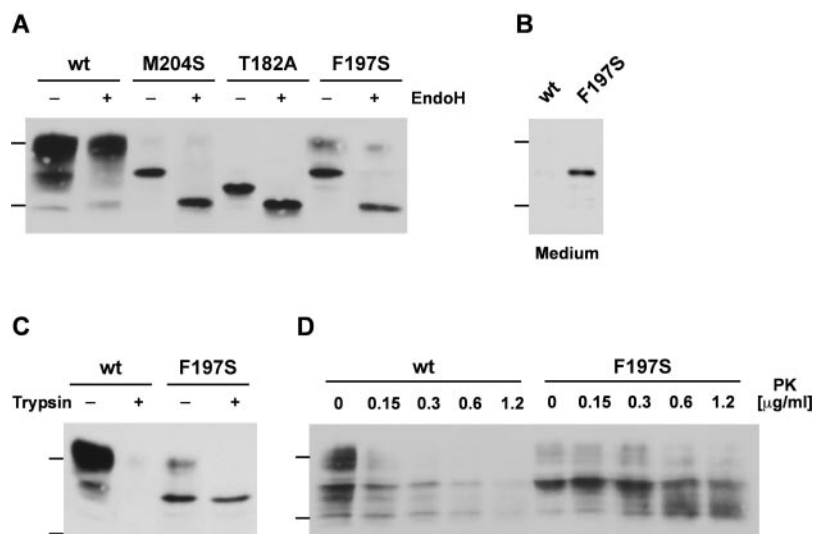


**FIG. 8. The pathogenic mutant F197S lacks the GPI anchor, adopts a partially protease-resistant conformation, and is secreted.** A, the pathogenic PrP mutant F197S interferes with complex glycosylation. Transiently transfected N2a cells were lysed and the extracts split into two aliquots. One aliquot was incubated with Endo H, the other was mock-treated. PrP was detected by Western blotting. B, F197S is secreted. Cells expressing wild type PrP (*wt*) or the F197S mutant were cultivated in serum-free medium for 3 h at 37 °C and PrP present in the cell culture medium (*Medium*) was detected by Western blotting. C, the majority of F197S is not present at the cell surface. Intact cells were incubated on ice with trypsin, lysed, and residual PrP was detected by Western blotting. As a control, mock-treated cells (*Trypsin* –) were analyzed in parallel. D, F197S adopts a partially protease-resistant conformation. Protein extracts from transiently transfected N2a cells were subjected to increasing concentrations of PK as indicated. Remaining PrP was detected by Western blotting. Molecular size markers are indicated as bars on the left side of the panels and represent 36 and 22 kDa.

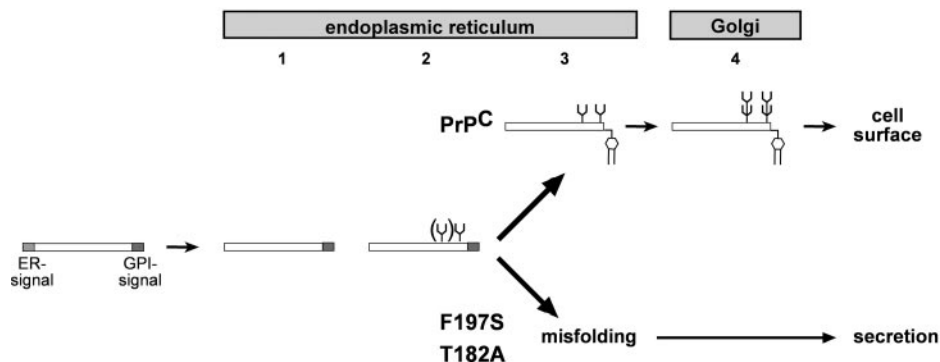


**FIG. 9. Two pathogenic mutations interfere with folding and maturation of PrP.** A schematic summary of the biogenesis of PrP<sup>C</sup> and pathogenic mutants linked to inherited prion diseases in humans. Maturation of PrP<sup>C</sup> is characterized by four distinct modifications: 1) cleavage of the N-terminal ER signal sequence; 2) addition of core glycans; 3) transfer of a GPI anchor (simultaneously with the cleavage of the C-terminal signal sequence); and 4) terminal processing of the glycans. Finally, PrP<sup>C</sup> is targeted to the outer surface of the plasma membrane. In contrast, the pathogenic mutations F197S and T182A severely affect folding and maturation of the prion protein. N-terminal signal sequence cleavage and core glycosylation occur, however, these mutants spontaneously adopt a misfolded conformation. Neither addition of the GPI anchor nor conversion of the core glycans into complex structures takes place. As a result, the pathogenic mutants are secreted as high mannose glycoforms.

pathogenic PrP mutants were not complex glycosylated. Based on previous studies we favor the explanation that the lack of a membrane anchor is responsible for the immature glycosylation status of the mutants. It is known that the type of membrane anchorage is not critical for the glycosylation status. Native GPI-anchored PrP<sup>C</sup> as well as PrP-CD4, a mutant with a heterologous C-terminal transmembrane domain, are both complex glycosylated (19, 42). However, when the GPI anchor addition is inhibited by mutating the acceptor amino acid within the GPI anchor signal sequence, the core glycans are not converted into complex structures (19). We therefore conclude that a membrane anchor is required for the terminal processing of the two PrP glycans.

**Abnormal PrP Conformers and Neurodegeneration**—Our study provides experimental evidence that two PrP mutants linked to inherited prion diseases in humans are devoid of a GPI anchor and are secreted. In view of the fact that PrP<sup>Sc</sup> contains a GPI anchor similarly to PrP<sup>C</sup> (8), the existence of secreted pathogenic PrP conformers might be unexpected. On

the other hand, a recent study indicated that recombinant PrP, expressed in bacteria and subsequently misfolded *in vitro*, can induce prion diseases in transgenic mice; of note, this recombinant PrP did not contain a GPI anchor (43). Other studies in transgenic mice revealed that even in the absence of infectious PrP<sup>Sc</sup>, PrP misfolding at the ER membrane or in the cytosol can induce neurodegeneration (44, 45). Importantly, some pathogenic mutations linked to inherited prion diseases in humans favor the formation of such aberrant ER topologies (44) or direct PrP into the cytosol (30). Based on these observations it is difficult to provide a unifying model explaining the neurotoxicity of misfolded PrP conformers. Thus, it is conceivable that pathogenicity is not restricted to a single PrP species; there might exist different pathogenic PrP conformers, derived from either infectious PrP<sup>Sc</sup> or mutant PrP, which can induce neuronal death by distinct pathways.

**Acknowledgment**—We are grateful to F. Ulrich Hartl for continuous support and helpful discussions.

## REFERENCES

- Aguzzi, A., Montrasio, F., and Kaeser, P. S. (2001) *Nat. Rev. Mol. Cell. Biol.* **2**, 118–126
- Collinge, J. (2001) *Annu. Rev. Neurosci.* **24**, 519–550
- Prusiner, S. B., Scott, M. R., DeArmond, S. J., and Cohen, F. E. (1998) *Cell* **93**, 337–348
- Weissmann, C., Fischer, M., Raeber, A., Büeler, H., Sailer, A., Shmerling, D., Rülke, T., Brandner, S., and Aguzzi, A. (1996) *Cold Spring Harbor Symp. Quant. Biol.* **61**, 511–522
- Spudich, S., Mastrianni, J. A., Wrensch, M., Gabizon, R., Meiner, Z., Kahana, I., Rosenmann, H., Kahana, E., and Prusiner, S. B. (1995) *Mol. Med.* **1**, 607–613
- Tatzelt, J., and Winklhofer, K. F. (2004) *Amyloid* **11**, 162–172
- Haraguchi, T., Fisher, S., Olofsson, S., Endo, T., Groth, D., Tarentino, A., Borchelt, D. R., Teplow, D., Hood, L., Burlingame, A., Lycke, E., Kobata, A., and Prusiner, S. B. (1989) *Arch. Biochem. Biophys.* **274**, 1–13
- Stahl, N., Borchelt, D. R., Hsiao, K., and Prusiner, S. B. (1987) *Cell* **51**, 229–240
- Lowe, M. E. (1992) *J. Cell Biol.* **116**, 799–807
- Stimson, E., Hope, J., Chong, A., and Burlingame, A. L. (1999) *Biochemistry* **38**, 4885–4895
- Rudd, P. M., Endo, T., Colominas, C., Groth, D., Wheeler, S. F., Harvey, D. J., Wormald, M. R., Serban, H., Prusiner, S. B., Kobata, A., and Dwek, R. A. (1999) *Proc. Natl. Acad. Sci. U. S. A.* **96**, 13044–13049
- Donne, D. G., Viles, J. H., Groth, D., Mehlhorn, I., James, T. L., Cohen, F. E., Prusiner, S. B., Wright, P. E., and Dyson, H. J. (1997) *Proc. Natl. Acad. Sci. U. S. A.* **94**, 13452–13457
- Riek, R., Hornemann, S., Wider, G., Billeter, M., Glockshuber, R., and Wuthrich, K. (1996) *Nature* **382**, 180–182
- Riek, R., Hornemann, S., Wider, G., Glockshuber, R., and Wuthrich, K. (1997) *FEBS Lett.* **413**, 282–288
- Riek, R., Wider, G., Billeter, M., Hornemann, S., Glockshuber, R., and Wuthrich, K. (1998) *Proc. Natl. Acad. Sci. U. S. A.* **95**, 11667–11672
- Nitrini, R., Rosenberg, S., Passos-Bueno, M. R., da Silva, L. S., Iughetti, P., Papadopoulos, M., Carrilho, P. M., Caramelli, P., Albrecht, S., Zatz, M., and LeBlanc, A. (1997) *Ann. Neurol.* **42**, 138–146
- Dlouhy, S. R., Hsiao, K., Farlow, M. R., Foroud, T., Conneally, P. M., Johnson, P., Prusiner, S. B., Hodes, M. E., and Ghetti, B. (1992) *Nat. Genet.* **1**, 64–67
- Gilch, S., Winklhofer, K. F., Nunziante, M., Lucassen, R., Spielhauer, C., Muranyi, W., Groschup, M. H., Riesner, D., Tatzelt, J., and Schätzl, H. M. (2001) *EMBO J.* **20**, 3957–3966
- Winklhofer, K. F., Heske, J., Heller, U., Reintjes, A., Muranji, W., Moarefi, I., and Tatzelt, J. (2003) *J. Biol. Chem.* **278**, 14961–14970
- Kacsak, R. J., Rubenstein, R., Merz, P. A., Tonna-DeMasi, M., Fersko, R., Carp, R. I., Wisniewski, H. M., and Diring, H. (1987) *J. Virol.* **61**, 3688–3693
- Winklhofer, K. F., and Tatzelt, J. (2000) *Biol. Chem.* **381**, 463–469
- Kiachopoulos, S., Heske, J., Tatzelt, J., and Winklhofer, K. F. (2004) *Traffic* **5**, 426–436
- Tatzelt, J., Prusiner, S. B., and Welch, W. J. (1996) *EMBO J.* **15**, 6363–6373
- Tatzelt, J., Groth, D. F., Torchia, M., Prusiner, S. B., and DeArmond, S. J. (1999) *J. Neuropathol. Exp. Neurol.* **58**, 1244–1249
- Rogers, M., Taraboulos, A., Scott, M., Groth, D., and Prusiner, S. B. (1990) *Glycobiology* **1**, 101–109
- Lehmann, S., and Harris, D. A. (1997) *J. Biol. Chem.* **272**, 21479–21487
- Rogers, M., Yehiely, F., Scott, M., and Prusiner, S. B. (1993) *Proc. Natl. Acad. Sci. U. S. A.* **90**, 3182–3186
- Blochberger, T. C., Cooper, C., Peretz, D., Tatzelt, J., Griffith, O. H., Baldwin, M. A., and Prusiner, S. B. (1997) *Protein Eng.* **10**, 1465–1473
- Winklhofer, K. F., Heller, U., Reintjes, A., and Tatzelt, J. (2003) *Traffic* **4**, 313–322
- Heske, J., Heller, U., Winklhofer, K. F., and Tatzelt, J. (2004) *J. Biol. Chem.* **279**, 5435–5443
- Yoshimori, T., Yamamoto, A., Moriyama, Y., Futai, M., and Tashiro, Y. (1991) *J. Biol. Chem.* **266**, 17707–17712
- Liemann, S., and Glockshuber, R. (1999) *Biochemistry* **38**, 3258–3267
- Vanik, D. L., and Surewicz, W. K. (2002) *J. Biol. Chem.* **277**, 49065–49070
- McCracken, A. A., and Brodsky, J. L. (2003) *Bioessays* **25**, 868–877
- Heller, U., Winklhofer, K. F., Heske, J., Reintjes, A., and Tatzelt, J. (2003) *J. Biol. Chem.* **278**, 36139–36147
- Winklhofer, K. F., Reintjes, A., Hoener, M. C., Voellmy, R., and Tatzelt, J. (2001) *J. Biol. Chem.* **276**, 45160–45167
- Tatzelt, J., Zuo, J. R., Voellmy, R., Scott, M., Hartl, U., Prusiner, S. B., and Welch, W. J. (1995) *Proc. Natl. Acad. Sci. U. S. A.* **92**, 2944–2948
- Dalley, J. A., and Bulleid, N. J. (2003) *J. Biol. Chem.* **278**, 51749–51757
- Wildegger, G., Liemann, S., and Glockshuber, R. (1999) *Nat. Struct. Biol.* **6**, 550–553
- Pless, D. D., and Lennarz, W. J. (1977) *Proc. Natl. Acad. Sci. U. S. A.* **74**, 134–138
- McCune, J. M., Fu, S. M., Kunkel, H. G., and Blobel, G. (1981) *Proc. Natl. Acad. Sci. U. S. A.* **78**, 5127–5131
- Taraboulos, A., Scott, M., Semenov, A., Avrahami, D., Laszlo, L., and Prusiner, S. B. (1995) *J. Cell Biol.* **129**, 121–132
- Legname, G., Baskakov, I. V., Nguyen, H. O., Riesner, D., Cohen, F. E., DeArmond, S. J., and Prusiner, S. B. (2004) *Science* **305**, 673–676
- Hegde, R. S., Mastrianni, J. A., Scott, M. R., DeFea, K. A., Tremblay, P., Torchia, M., DeArmond, S. J., Prusiner, S. B., and Lingappa, V. R. (1998) *Science* **279**, 827–834
- Ma, J., Wollmann, R., and Lindquist, S. (2002) *Science* **298**, 1781–1785
- Kraulis, P. (1991) *J. Appl. Crystallogr.* **24**, 946–950
- Merrit, E. A., and Bacon, D. J. (1997) *Methods Enzymol.* **277**, 505–524

**Pathogenic Mutations Located in the Hydrophobic Core of the Prion Protein Interfere with Folding and Attachment of the Glycosylphosphatidylinositol Anchor**

Sophia Kiachopoulos, Andreas Bracher, Konstanze F. Winklhofer and Jörg Tatzelt

*J. Biol. Chem.* 2005, 280:9320-9329.

doi: 10.1074/jbc.M412525200 originally published online December 10, 2004

---

Access the most updated version of this article at doi: [10.1074/jbc.M412525200](https://doi.org/10.1074/jbc.M412525200)

Alerts:

- [When this article is cited](#)
- [When a correction for this article is posted](#)

[Click here](#) to choose from all of JBC's e-mail alerts

This article cites 47 references, 26 of which can be accessed free at <http://www.jbc.org/content/280/10/9320.full.html#ref-list-1>